ADVANCED FUNCTIONAL MATERIALS
www.afm-journal.de

Energy Transfer to a Stable Donor Suppresses Degradation in Organic Solar Cells

*Andreas Weu, Rhea Kumar, Julian F. Butscher, Vincent Lami, Fabian Paulus, Artem A. Bakulin, and Yana Yaynzof**

Despite many advances toward improving the stability of organic photovoltaic devices, environmental degradation under ambient conditions remains a challenging obstacle for future application. Particularly conventional systems employing fullerene derivatives are prone to oxidize under illumination, limiting their applicability. Here, the environmental stability of the small molecule donor DRCN5T together with the fullerene acceptor $PC_{70}BM$ is reported. It is found that this system exhibits exceptional device stability, mainly due to almost constant short-circuit current. By employing ultrafast femtosecond transient absorption spectroscopy, this remarkable stability is attributed to two separate mechanisms: 1) DRCN5T exhibits high intrinsic resistance toward external factors, showing no signs of deterioration. 2) The highly sensitive $PC_{70}BM$ is stabilized against degradation by the presence of DRCN5T through ultrafast, long-range energy transfer to the donor, rapidly quenching the fullerene excited states which are otherwise precursors for chemical oxidation. It is proposed that this photoprotective mechanism be utilized to improve the device stability of other systems, including nonfullerene acceptors and ternary blends.

1. Introduction

Organic photovoltaics (OPVs) have seen rapid performance improvements in the last five years, now achieving power conversion efficiencies (PCEs) of 16%.[1,2] While most OPV devices incorporate polymers as donor materials, there is an increasing interest in applying solution-processible small molecules as both the donor and acceptor components of the bulk heterojunction (BHJ) active layer. This is motivated by their easy purification, small batch-to-batch variation and improved stability relative to polymer materials.[3–7] The application of small molecules as non-fullerene acceptors (NFAs) is already common, the emergence of which resulted in an unexpected surge in device performance.[8–14] Fewer examples exist of small molecules applied as donor materials,[15,16] but efficiencies surpassing 10% have been demonstrated.[17,18]

With increasing performances, offering OPVs as a promising candidate for industrial application, the remaining challenge of low operational stability precludes their large-scale integration into the PV market. The degradation mechanisms of polymer:fullerene-based solar cells have been a focus of extensive study in the last decade and are now reasonably well understood. Under illumination, polymer solar cells typically show a strong initial decrease in device performance ("burn-in"), caused by formation of defects in the bandgap.[19–22] In addition, exposure to oxygen leads to p-type doping in some polymer systems, which causes increased bimolecular recombination or formation of traps which in turn impede charge generation and transport.[23–26] The combined influence of oxygen and light induces irreversible photo-oxidation in many polymers through reactions involving singlet oxygen or radical superoxide, causing chemical decomposition and deactivation of the chromophores.[27–29] Morphological changes induced by elevated temperatures under operating conditions provide another degradation pathway. It has been shown that exposure to light or high temperatures causes demixing of the phases thus reducing propensity for charge separation, often accelerated by the presence of processing additives like 1,8-diiodooctane (DIO).[19,30–33] Foremost of all, fullerene acceptors are usually the main factor limiting the device lifetime. The most used derivatives $PC_{60}BM$ and $PC_{70}BM$ have been reported to dimerize or degrade upon exposure to oxygen and light, which limits device performance due to trap formation or a reduction in electron mobility.[34–37] Therefore, investigating strategies to suppress the degradation in fullerene-based organic solar cells is imperative for future utilization of such devices.

A. Weu, J. F. Butscher, Dr. V. Lami, Dr. F. Paulus, Prof. Y. Vaynzof
Kirchhoff Institute for Physics and the Centre for Advanced Materials
Im Neuenheimer Feld 227, 69120 Heidelberg, Germany

J. F. Butscher, Dr. V. Lami, Dr. F. Paulus, Prof. Y. Vaynzof
Integrated Centre for Applied Physics and Photonic Materials and Centre for Advancing Electronics Dresden (cfaed)
Technical University of Dresden
Nöthnitzer Straße 61, 01187 Dresden, Germany
E-mail: yana.vaynzof@tu-dresden.de

R. Kumar, Dr. A. A. Bakulin
Centre for Plastic Electronics
Department of Chemistry
Imperial College London
London SW7 2AZ, UK

The ORCID identification number(s) for the author(s) of this article can be found under https://doi.org/10.1002/adfm.201907432.

DOI: 10.1002/adfm.201907432

In contrast to polymer:fullerene systems, the stability of OPVs that employ small molecule (SM) donors has attracted little attention so far. Early work investigated the influence of water and oxygen in zinc phthalocyanine-based solar cells, but identified either the low work function electrodes and transport layers in the standard architecture or the C_{60} acceptor as the main factors for device failure.[38–40] While the poor stability of standard architecture devices in air is known,[38,41–44] inverted architecture SM OPVs have been reported to be relatively stable, but no justification of this difference or underlying degradation mechanism has been reported.[45]

The stability of "new-generation" small molecule donors is even less well studied. One particularly interesting small molecule donor 2,2′- [(3,3‴,3‴″,4′-tetraoctyl[2,2′:5′,2″:5″,2‴:5‴,2‴″-quinquethiophene]-5,5‴″-diyl) bis[(Z)-methylidyne(3-ethyl-4-oxo-5,2-thiazolidinediylidene)]] bis-propanedinitrile (DRCN5T) was first designed and synthesized by Y. Chen and co-workers in 2015.[46] This donor SM has been shown to result in impressive performance with the fullerene acceptor [6,6]-Phenyl-C70-butyric acid methyl ester ($PC_{70}BM$) as well as several NFAs.[47–49] The stability of various standard architecture SM OPVs (including DRCN5T: $PC_{70}BM$) has been analyzed by Cheacharoen et al. who showed that heating the films, either on a hotplate or during exposure to visible light, leads to a significant burn-in within 100 h, attributed to morphological changes in the nanostructure of the blend.[50] Similar results were obtained by Min et al. who investigated the stability of encapsulated standard architecture DRCN5T:$PC_{70}BM$ devices with a focus on the role of the active layer microstructure on the degradation dynamics.[51] However, while previous studies focused on heat-induced effects on the small-scale morphology in inert conditions, the influence of oxygen on the operation of DRCN5T:$PC_{70}BM$ devices is hitherto unreported. A detailed understanding of the environmental stability in ambient atmosphere is highly relevant as current encapsulation techniques are expensive and either incompatible with flexible substrates or insufficiently impermeable to oxygen or water.

In this work, we demonstrate that the representative SM system DRCN5T:$PC_{70}BM$ exhibits superior stability in oxygenated environment and under 1 Sun illumination relative to many other polymer:$PC_{70}BM$ OPV systems. We show that the use of DRCN5T donor provides a photoprotective mechanism that suppresses the degradation of the fullerene acceptor. This photoprotective effect is enabled by two factors: 1) the intrinsically high photostability of the donor molecule, even in the presence of oxygen, and 2) efficient and ultrafast energy transfer from the $PC_{70}BM$ acceptor to the donor SM, which effectively quenches the high energy excited state on the fullerene, preventing its photo-oxidation. It is noteworthy that recent reports have identified fullerene degradation as a major limitation to the stability of OPV devices,[27,52,53] highlighting the importance of developing mitigation strategies such as the photoprotection realized herein. By applying ultrafast femtosecond (fs) transient absorption (TA) spectroscopy, we examine the processes governing charge generation in both pristine and degraded solar cells and demonstrate how efficient charge generation is maintained upon exposure to oxygen and light. Finally, we discuss how this photoprotective mechanism can be exploited in future small molecule OPV devices.

2. Results

The chemical structures of DRCN5T and $PC_{70}BM$, along with the schematic inverted architecture structure of the investigated solar cells are illustrated in **Figure 1**a. Although reports highlighting problems with the common extraction layers MoO_x/Ag exist,[54–56] this structure with high work function contacts was chosen to minimize degradation effects by the electrodes and allowed us to focus on the processes affecting the active layer.[26,45] In this architecture, cesium-doped zinc-oxide (ZnO:Cs) served as electron transport/hole blocking layer[57,58] and molybdenum-oxide (MoO_x) as hole transport/electron blocking layer; indium tin oxide (ITO) and silver acted as the contacts. In this first report of the application of DRCN5T:$PC_{70}BM$ in an inverted device architecture we were able to achieve a maximum PCE of 8.2%, competitive with previously reported standard architecture devices.[46,51] The bandgaps and highest occupied molecular orbital (HOMO) energy levels of the active components with respect to vacuum level have been measured by ultraviolet photoelectron spectroscopy (UPS) and UV–vis absorption spectroscopy (Figure 1b). In the energy level diagram, arrows indicate electron transfer from donor to acceptor and a possible energy transfer from acceptor to donor, facilitated by overlapping absorption and emission of DRCN5T and $PC_{70}BM$ (Figure 1c).

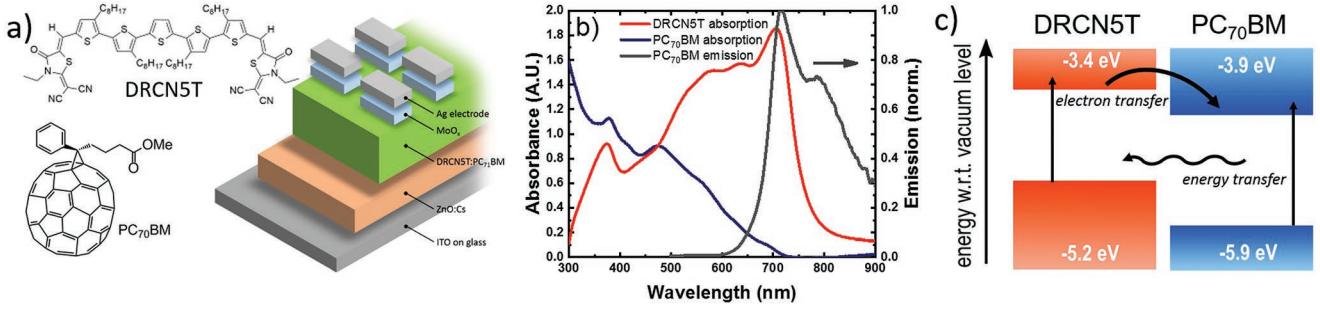

Figure 1. a) Chemical structures of the small molecule DRCN5T together with the fullerene $PC_{70}BM$. The inverted architecture solar cell comprising the active layer sandwiched between the ZnO electron transporting layer and MoO_x hole transporting layer. b) Absorption spectra of DRCN5T and $PC_{70}BM$ and emission spectrum of $PC_{70}BM$. c) Energy level diagram of the active layer with arrows indicating photon absorption, charge transfer at the interface, and energy transfer between the materials.

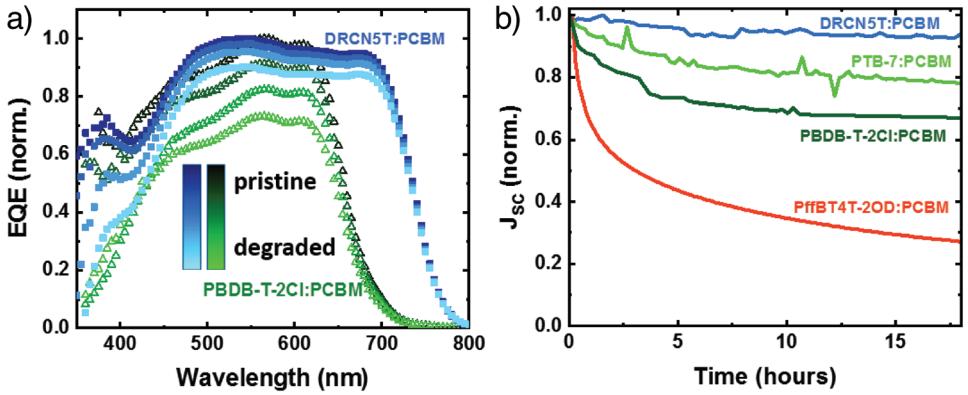

Figure 2. a) Evolution of EQE spectra for DRCN5T:$PC_{70}BM$ and PBDB-T-2Cl:$PC_{70}BM$ solar cells upon exposure to light and oxygen for 22 h. b) Reduction in J_{SC} of DRCN5T:$PC_{70}BM$ as compared to three analogous polymer:fullerene OPV systems.

To investigate the stability of this SM system upon exposure to oxygen and light, the performances of 24 DRCN5T:$PC_{70}BM$ solar cells were monitored for 22 h under continuous illumination conditions of 1 Sun and a controlled atmosphere of 20% O_2 in a bespoke environmental setup.[26] This setup ensures a constant flow of gas to minimize heating of the substrates with the temperature of the gas being continuously evaluated.

Figure 2a shows the effect of the aforementioned degradation conditions on the external quantum efficiency (EQE) spectra of the devices, acquired in situ. The response within the spectral range of 450–800 nm, arising predominantly from the contribution of the donor, shows only a very minor decrease. A minor photobleaching of DRCN5T, which can be caused by oxygen-induced radical formation or light-induced chemical modifications of the molecular structure,[59–61] is mostly suppressed when integrating the molecule into a blend with $PC_{70}BM$ (Figure S1, Supporting Information). This stabilization is caused by the rapid quenching of donor excitons by charge transfer to the acceptor.[37,62] The decrease in EQE is more noticeable at wavelengths below 410 nm where $PC_{70}BM$ also contributes to current generation. Here, a clear reduction in the EQE is observed which cannot be correlated to the reduction of optical absorption (Figure S1, Supporting Information). However, the overall decrease in quantum efficiency is unusually small when compared to other OPVs employing fullerene acceptors. For comparison, we show the EQE evolution of poly [(2,6-(4,8-bis(5-(2-ethylhexyl-3-chloro)thiophen-2-yl)-benzo] [1,2-b:4,5-b']dithiophene))-*alt*-(5,5-(1′,3′-di-2-thienyl-5′,7′-bis(2-ethylhexyl)benzo [1′,2′-c:4′,5′-c′]dithiophene-4,8-dione) (PBDB-T-2Cl):$PC_{70}BM$ solar cells degraded under identical conditions. For this system, a strong reduction of the EQE is observed, as is typical for polymer:fullerene OPVs. To highlight the superior stability of DRCN5T:$PC_{70}BM$, the decrease of short-circuit current (J_{SC}) over time is compared to other high efficiency polymer:fullerene systems (Figure 2b). The benchmark materials poly[(5,6-difluoro-2,1,3-benzothiadiazol-4,7-diyl)-*alt*-(3,3‴-di(2-octyldodecyl)-2,2′,5′,2″,5″,2‴-quaterthiophen-5,5‴-diyl)] (PffBT4T-2OD), poly [4,8-bis] [(2-ethylhexyl)oxy] benzo [1,2-b:4,5-b′]dithiophene-2,6-diyl [3-fluoro-2-] [(2-ethylhexyl)carbonyl]thieno [3,4-b]thiophenediyl [1,2] (PTB-7), and PBDB-T-2Cl, each with $PC_{70}BM$ as the acceptor, have been chosen as a comparison. While all polymer systems, particularly PffBT4T-2OD, show significant burn-in through loss of J_{SC}, the J_{SC} of DRCN5T:$PC_{70}BM$ maintains over 90% after 18 h of degradation, in agreement with the small reduction of the EQE. To highlight the unusually stable current generation in DRCN5T:$PC_{70}BM$, we compare the results to a reference measurement taken in nitrogen under dark conditions (Figure S2, Supporting Information), in which no reduction in J_{SC} was observed.

Both the spectral position and the low extent of the EQE reduction indicate that degradation in this system is effectively suppressed and mostly depletes photocurrent generated due to absorption by the $PC_{70}BM$ molecules. Femtosecond transient absorption spectroscopy was therefore carried out in order to investigate the effect of degradation on the exciton and charge carrier dynamics of the system.

In a first experiment, the kinetics of neat films of DRCN5T and $PC_{70}BM$ were investigated (**Figure 3**); corresponding spectra and un-normalized data can be found in Figure S3 (Supporting Information). A singular value decomposition (SVD) analysis was performed on the data which yielded a single dominant component for the DRCN5T film, assigned to donor excitons. After excitation with a 700 nm pump pulse, excitons are created within the time resolution of the setup (80 fs) and recombine within 300 ps. No effect of degradation is observed in the exciton dynamics throughout the 9 h of degradation (Figure 3a), apart from ≈20% loss of absorption due to photobleaching (see Figure S3, Supporting Information), demonstrating the intrinsically high stability of DRCN5T.

In the neat $PC_{70}BM$ film, excitons were created by a 350 nm pump pulse (Figure 3b). Prior to degradation, the excitons decay with a lifetime of 50 ps. However, continuous exposure to oxygen and light for 7 h causes a notable reduction of exciton lifetime to 7 ps. After a pump-probe delay of 300 ps this trend inverts as a marginally larger exciton amplitude with increasing degradation is observed. We speculate that the initial reduction of the signal followed by an increase at later times corresponds to the formation of trap states as a consequence of degradation, efficiently quenching the excitons and creating long-lived, trapped charges, previously observed in systems containing $PC_{70}BM$.[26] Accordingly, the spectrum between 800 nm and 1250 nm changes gradually

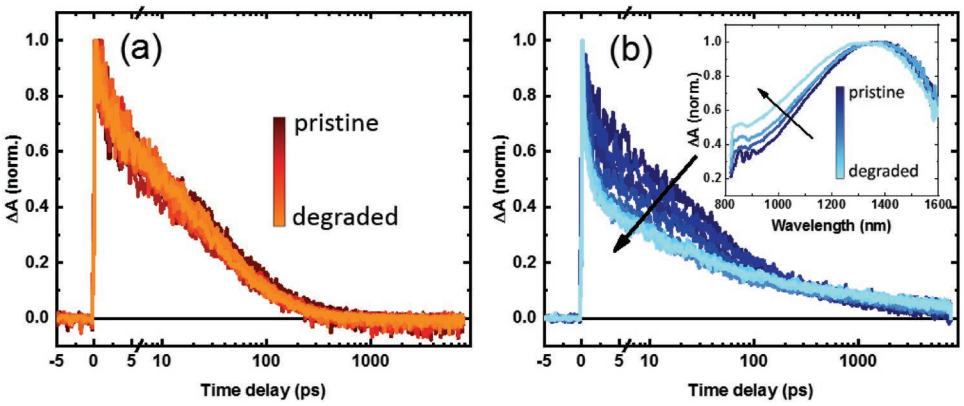

Figure 3. Transient absorption data for the neat materials in the studied blend. a) Kinetics of DRCN5T excitons (excited at 700 nm with 150 nJ, probed at 1200 nm) do not change upon degradation for 9 h. b) Kinetics of $PC_{70}BM$ excitons (excited at 350 nm with 150 nJ, probed at 1350 nm) show greater early quenching of excitons with increased degradation for 7 h. Inset: spectral change indicating the formation of trapped species.

during exposure to oxygen and light (see inset Figure 3b), indicating the formation of a second species, likely to be trapped carriers.

Having investigated the stability of the constituent materials, we turn our attention to the degradation of the OPV blend system. Upon selectively exciting the donor molecule with 700 nm pump pulses, two distinct contributions to the blend spectrum, assigned to DRCN5T excitons and free charge carriers, were extracted by global analysis (**Figure 4**). The spectrum of the DRCN5T exciton created directly by the pump pulse is visibly unaffected by exposure to light and oxygen (Figure 4a). The kinetics shown in Figure 4b confirm this stability, with approximately consistent exciton decay lifetimes which vary slightly but without correlation to degradation (see Figure S6, Supporting Information). The lifetime of donor excitons in the blend is intuitively shorter than that in neat DRCN5T due to quenching by charge transfer at the donor:acceptor interface. The kinetics associated with the second component reveal that free charge carriers form on a 10 ps timescale, concomitantly with the decay of excitons (Figure 4d). The charges are characterized by a long-lived signal (>8ns), suggesting that recombination is primarily of a bimolecular nature. The

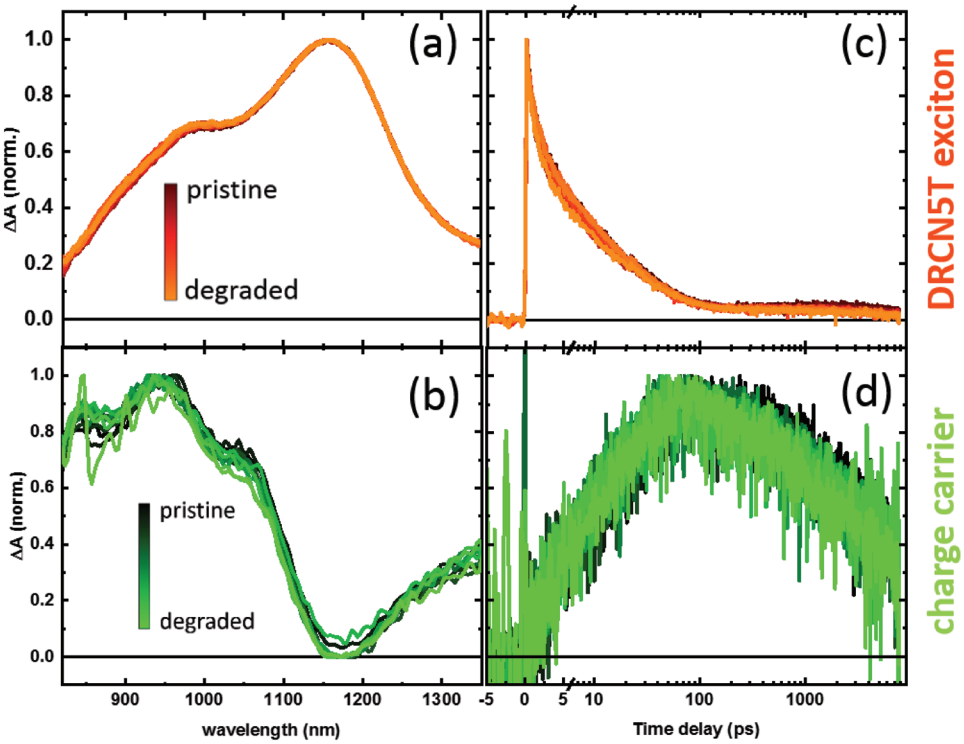

Figure 4. Spectra (left) and kinetics (right) of global analysis (GA) derived components of the transient absorption spectrum of the DRCN5T:$PC_{70}BM$ blend after 700 nm excitation (150 nJ) at selected stages of the degradation process. a) DRCN5T exciton and b) charge spectra show no signs of degradation. c) Exciton and d) charge kinetics are unchanged by degradation over 5 h in air and a constant illumination of 1 Sun.

spectrum of charges formed in the blend remains unchanged during degradation (Figure 4c), with lifetimes of charge generation and decay processes showing no clear trends during the degradation experiments (Figure S6, Supporting Information). Taken together, these observations suggest that the processes of exciton formation in DRCN5T, diffusion to an interface and subsequent charge separation by electron transfer to $PC_{70}BM$ are unaffected by degradation throughout the duration of the experiment. In contrast to the neat materials, no change in absorption is observed (Figure S4, Supporting Information) suggesting a stabilizing influence of the blend environment on the excitons, most likely due to fast quenching of high energy excitations on the donor by the presence of the acceptor.[37,62] This observation is in excellent agreement with the very small reduction of EQE and J_{SC} observed in degraded devices (Figure 2).

In order to investigate the role of the fullerene on the photophysical behavior of the blend, TA of DRCN5T:$PC_{70}BM$ was carried out using a 350 nm pump pulse for selective excitation of the acceptor. The normalized decay in amplitude of the resultant spectra at the selected wavelength of 1350 nm, representing the maximum absorption of the $PC_{70}BM$ exciton, are shown for neat $PC_{70}BM$ (**Figure 5**a) and for DRCN5T:$PC_{70}BM$ (Figure 5b) films. We note that a control experiment in neat DRCN5T (Figure S5, Supporting Information) shows only a minor response of the donor to the 350 nm pulse. Therefore, the signal at 1350 nm in the blend contains also small contributions from the donor exciton. The effect of degradation is striking for the neat acceptor film, while the blend kinetics reveal this degradation is strongly suppressed in the blend. Although the presence of charge transfer in the blend complicates the data interpretation, we emphasize that the fast (sub 2 ps) component present in degraded $PC_{70}BM$ does not appear in the blend even after long time exposure to air and light. This observation confirms that the products of $PC_{70}BM$ photodegradation are significantly minimized in the blend.

As DRCN5T has proven stable both in pristine and blended environments, our results raise the question of the mechanism actively preventing the degradation of $PC_{70}BM$ when blended with DRCN5T. In order to elucidate the origin of this remarkable enhancement in stability of the blend over its components, transient absorption spectra were also recorded following a 250 nm excitation. At this wavelength, a far larger fraction of $PC_{70}BM$ is excited relative to DRCN5T as the absorption of the donor is minimal in comparison. Three components result from spectral reconstruction with global analysis (**Figure 6**). Note that the used genetic algorithm is unable to fully separate the signals of fullerene excitons and free charges, explaining the unusual shape of the spectral profile. As demonstrated in the normalized kinetics, only the $PC_{70}BM$ exciton is generated by pump excitation. In contrast, the formation of the DRCN5T exciton is not initiated by the pump pulse, but instead occurs concurrently with $PC_{70}BM$ exciton decay, indicating the manifestation of efficient energy transfer from the acceptor to the donor on the sub-picosecond timescale. Based on these observations we propose the following model (illustrated in Figure 6c) to rationalize the stabilizing nature of the blend. Excitation of $PC_{70}BM$ leads to the formation of acceptor excitons which undergo an ultrafast (≈500 fs) and long-range energy transfer to DRCN5T, enabled by spectral overlap of $PC_{70}BM$ emission and DRCN5T absorption (Figure 1). This energy transfer occurs on a far faster timescale than a hole transfer from acceptor to donor which typically occurs on the ≈10 ps timescale. The resulting donor exciton diffuses to an interface where it subsequently dissociates into long-lived charge carriers after 100 ps. Since DRCN5T is intrinsically stable, the energy transfer does not lead to its degradation and rather facilitates efficient photoprotection of the fullerene. We note that while we measure no effects of degradation on the DRCN5T exciton, the determination of an exact origin of this intrinsic stability is beyond the scope of this work. These observations show that exciton formation and diffusion, electron transfer at the interfaces, and charge separation in DRCN5T:$PC_{70}BM$ devices is unaffected by the presence of oxygen or light. However, the observation of a stable short-circuit current implies that also the transport of charges to the electrodes remains largely unaffected, suggesting no significant changes to the active layer microstructure. To confirm this, we employed 2D-XRD measurements to determine the microstructure and crystallinity of the blend before and after degradation (Figure S7a,b, Supporting Information). The results show no substantial changes in the microstructure due to the degradation in oxygen and light for 20 h, from which we conclude that that electron and hole transport through the active layer remain stable throughout the

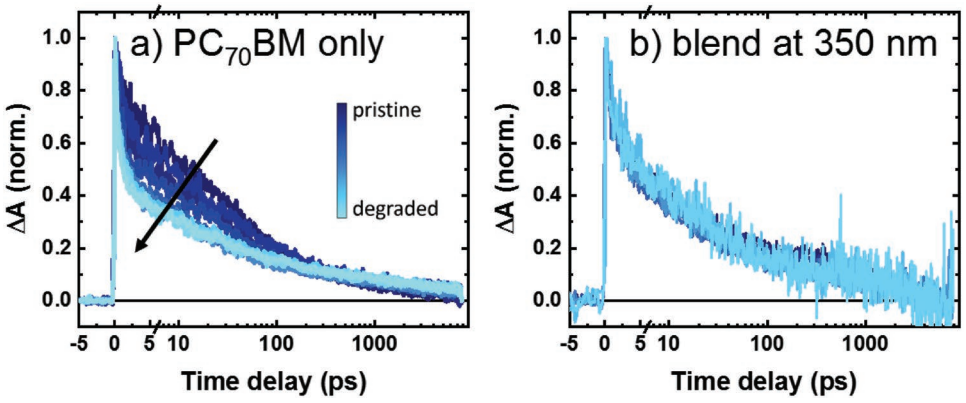

Figure 5. Normalized decay in amplitude of a) neat $PC_{70}BM$ and b) DRCN5T:$PC_{70}BM$ blend spectra excited with a 350 nm pump pulse (150 nJ) at the selected wavelength of 1350 nm at increasing extents of degradation.

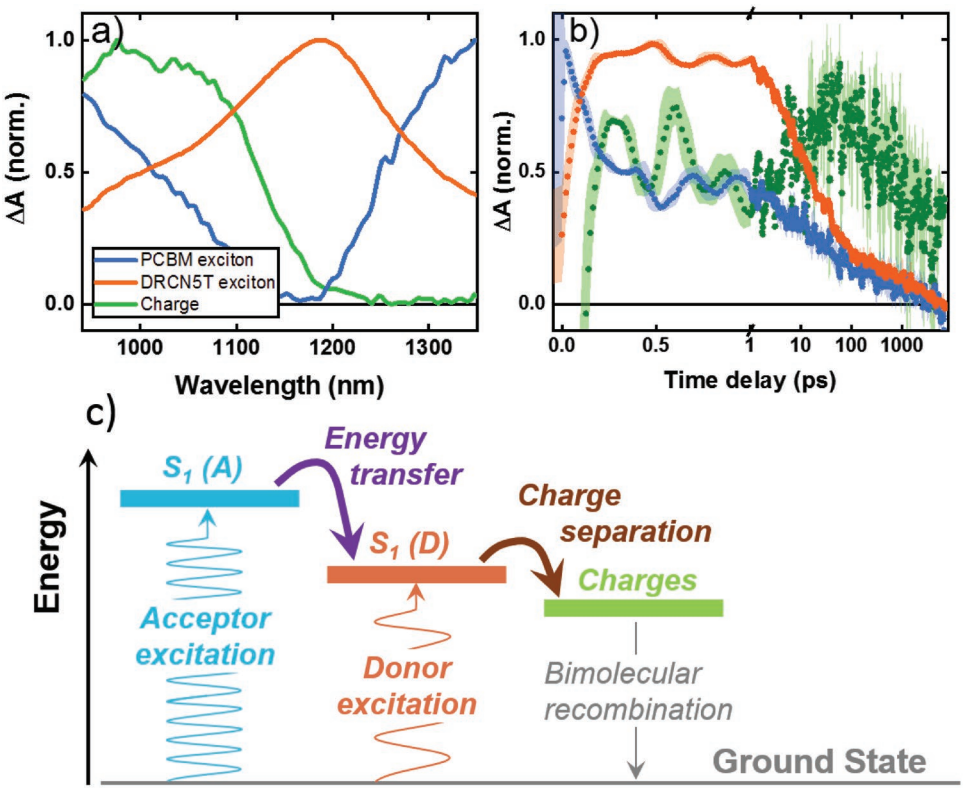

Figure 6. Normalized spectra a) and kinetics b) for the three contributions to the TA spectrum of DRCN5T:$PC_{70}BM$ after 250 nm excitation (150 nJ): acceptor exciton (blue), donor exciton (red), and free charges (green). Kinetic traces are plotted as moving averages with associated errors shown. c) Proposed model of energy transfer from $PC_{70}BM$ to DRCN5T prior to charge transfer.

entire experiment and oxygen exposure. Furthermore, transient photocurrent (TPC) kinetics were measured to analyze the extraction dynamics at the interlayers/electrodes (Figure S7c, Supporting Information). We find no correlation between extraction time (typically influenced by the presence of deep traps) and degradation, indicating that charge extraction across the interfaces to the transport layers and electrodes is predominantly unaffected by oxygen or light.

3. Discussion

The proposed energy transfer can be rationalized by a Förster-type process. The corresponding Förster radius depends mainly on the spectral overlap of emission and absorption of the two components (Figure 1). Assuming isotropic orientation of the dipoles ($\kappa^2 = 2/3$), a refraction index of $n = 1.5$, and the PL quantum yield of the fullerene to be $\Phi = 0.01\%$, the Förster radius is on the order of $R_0 = 1.6$ nm, in agreement with reports on other systems.[63–65] Taking the lifetime of the fullerene exciton in the absence of DRCN5T of 50 ps (Figure 3b) and assuming a mean distance between exciton and interface of 5 nm, this equates to a rate of $k_{ET} = 1.5 \times 10^7$ s^{-1} in the dipole–dipole approximation, according to Förster theory.

The presence of an efficient, ultrafast energy transfer has fascinating implications for the photophysics of this material system. In this case, the excitation of fullerene molecules does not result in a hole transfer to the donor, since charge transfer occurs on a timescale of ≈10 ps, while energy transfer is far faster, on a sub-ps timescale. It is important to note that this does not prevent the acceptor from contributing to photocurrent. Instead photocurrent is generated through electron transfer from the donor that follows the energy transfer process. By designing novel photovoltaic systems with complementary absorption to facilitate such energy transfer, one can maintain the contributions of both active layer components, while eliminating the limitations originating from the instability of fullerene or other wide-bandgap acceptors. Energy transfer also makes materials insensitive to the rate of hole transfer and allows to focus the material design exclusively on the optimization of electron transfer. Additionally, long-range energy transfer can assist in current generation by directed exciton transport to a donor:acceptor interface in contrast to range-limited, random exciton diffusion.[63]

The combination of the energy transfer from the acceptor with an ultrastable donor, like in DRCN5T:$PC_{70}BM$, results in both the charge generation and transport/extraction mechanisms remaining largely unaffected upon prolonged exposure to oxygen and light. Consequently, the J_{SC} in such a material system remains very stable over an extended period of time, in stark contrast to conventional OPV systems. We believe that the observed photoprotective effect of energy transfer from acceptor to donor can be further exploited in other systems and should influence design rules toward more stable devices. Current research focuses exclusively on the development of novel photovoltaic systems with efficient charge generation in which

the process of charge transfer places a key role. Our work demonstrates that the selection of active components must be done with consideration also of complementary absorption and emission spectra, as long-range energy transfer can stabilize the blend via ultrafast quenching of the excited state which would otherwise lead to rapid degradation of the material. Such a photoprotective effect essentially relaxes the stability requirement to only one of the blend components, while the other, higher bandgap, material can be less stable and yet remain protected. This effect could be particularly useful for NFAs with a low electron affinity which enable high V_{OC} but simultaneously facilitate formation of radical oxygen species by electron transfer.[66–68] We further propose that the stabilizing character of DRCN5T or similarly stable materials can be further capitalized in other systems employing unstable acceptors, for example by incorporating it as a third component in a ternary blend.[69] A preliminary experiment in PBDB-T-2Cl:$PC_{70}BM$ solar cells showed that the stability of J_{SC} can be increased by 15% upon the addition of 20% DRCN5T to the blend (Figure S8, Supporting Information).

4. Conclusion

In this work, we conclude that the SM:fullerene system DRCN5T:$PC_{70}BM$ is remarkably stable under continuous illumination in oxygenated conditions, evidenced by an unprecedentedly consistent J_{SC}. We rationalize this observation with two arguments: 1) DRCN5T itself is photophysically very stable and shows no signs of degradation aside from a minor photobleaching effect which is mitigated in the blend. 2) The inherent instability of $PC_{70}BM$ is overcome by ultrafast energy transfer from the fullerene to the small molecule, preventing the otherwise detrimental effect of high-energy excitations on the acceptor. These results highlight the superior stability of small molecule OPV materials, which should influence future strategy in the pursuit of efficient and stable material systems. Furthermore, consideration of complementary donor and acceptor molecules for design of blends that are specifically capable of ultrafast, long-range energy transfer can greatly improve the stability of the entire system. Finally, incorporation of DRCN5T into a ternary blend consisting of high-bandgap materials could lead to a much more stable device performance. To conclude, we propose that the synthesis of stable donors that complement the emission range of acceptor molecules is a viable route for the development of novel organic photovoltaic devices with superior efficiency and stability.

5. Experimental Section

Materials: DRCN5T and $PC_{70}BM$ were purchased from Ossila and Solenne. Zinc acetate dihydrate as a precursor to ZnO was bought from Sigma-Aldrich. All the materials were used as received without further purification.

Fabrication Organic Solar Cells: The investigated organic solar cells were fabricated on precut glass substrates, patterned with ITO as bottom electrode (PsiOTec Ltd., UK). After cleaning by subsequent sonication in acetone and isopropanol the substrates were transferred to a plasma cleaner for oxygen treatment. For inverted architecture devices, a thin ZnO layer (≈50 nm) was spin-coated from solution and annealed for 30 min at 200 °C based on previously reported procedures.[57,58] The active layer with a thickness of 100 nm was spin-coated from a chloroform solution of mixed DRCN5T:$PC_{70}BM$ in a weight ratio of 15 mg mL^{-1}:12.5 mg mL^{-1}. After thermal annealing for 10 min at 120 °C on a hotplate and subsequent solvent vapor annealing for 60 s in a Petri dish with saturated chloroform atmosphere, the substrates were transferred into a thermal evaporator (10^{-7} mbar) for deposition of 10 nm MoO_3 and 80 nm Ag.

Environmental Rig: For all oxygen degradation studies, the organic solar cells were prepared the same way as mentioned above, stored in a nitrogen filled glove box, and transferred to a sealed environmental box without exposure to ambient air. A constant flow of nitrogen was connected to the environmental box. The oxygen percentage was controlled by adjusting the relative flow rate of O_2 to N_2, and was continuously monitored by a zirconia sensor (Cambridge Sensotec, Rapidox 2100). All the samples were aged under simulated AM 1.5 sunlight at 100 mW cm^{-2} irradiance (ABET Sunlite 11002 solar simulator).

Current–Voltage (J–V) Measurements: Current density–voltage (*J–V*) characteristics of the photovoltaic devices were measured using a Keithley 2450 Source Measure Unit. *J–V* curves of the photovoltaics were recorded under an AM 1.5 G light illumination (100 mW cm^{-2}) using an ABET Sunlite 11002 solar simulator, which was adjusted in intensity to compensate for the spectral mismatch between the spectral output and the spectral response of both the DRCN5T:$PC_{70}BM$ device and the reference Si cell (NIST traceable, VLSI).

EQE: The EQE was measured with the monochromatic light of a halogen lamp from 350 to 800 nm, which was calibrated with a NIST-traceable Si diode (Thorlabs).

UV–Vis Absorption Spectroscopy: Films of DRCN5T and $PC_{70}BM$ (15 mg mL^{-1} and 12.5 mg mL^{-1} respectively) were spin-coated on glass substrates in a N_2-filled glove box and measured at room temperature with a JASCO UV-Vis V670 spectrometer.

Transient Absorption (Pump-probe) Spectroscopy: Samples for TA measurements were prepared identically to the active layers of solar cells. Since this system does not exhibit electric-field-induced charge generation,[70] all measurements were performed on active layer films and reference films of the BHJ components. Seed pulses (800 nm, < 100 fs) were generated at a repetition rate of 4 kHz by a Ti:Sapphire regenerative amplifier (Spectra-Physics Solstice, Newport Corporation), and routed toward an optical parametric amplifier (TOPAS, Light Conversion) to provide the pump. The seed pulses were also routed toward a mechanical delay stage in a commercially available femtosecond transient absorption spectrometer (HELIOS, Ultrafast Systems). Therein, the pump (modulated at 2 kHz) and the broadband near-infrared (≈800–1450 nm) probe were focused onto a ≈0.1 mm^2 spot on the sample. Analyses were performed in Origin and MATLAB. The degradation of the films during the TA measurements was approximated by focusing a white light LED (Thorlabs MWWHD3) onto the measurement spot, where an intensity of 100 mW cm^{-2} was assured by a silicon reference diode (NIST traceable, VLSI). The measurements were performed on unencapsulated films in the dry atmosphere of the optical lab.

Photoemission Spectroscopy: Films of DRCN5T and $PC_{70}BM$ (15 mg mL^{-1} and 12.5 mg mL^{-1}, respectively) were spin-coated on glass/ITO/ZnO substrates in a N_2-filled glove box. UPS measurements were performed using a double-differentially pumped He discharge lamp ($h\nu$ = 21.22 eV) with a pass energy of 2 eV. During data collection the samples were biased at −5 V in order to measure the onset of the secondary electrons.

Transient Photocurrent: For transient photocurrent measurements, the light of an inorganic LED (Thorlabs TO-1 3/4, λ = 465 nm) was pulsed by a function generator (Agilent/Keysight 33510B) and focused on the solar cell. An oscilloscope (Picoscope 5443A) with a 50 Ω terminator placed across the oscilloscope input was used to measure the transient photocurrent.

XRD: XRD measurements of the films on glass/ITO substrates were conducted on a Rigaku SmartLab diffractometer with a 9 kW rotating copper anode, equipped with a 0.5 mmϕ collimator. The 2D diffraction

pattern was collected with a HyPix3000 detector at a sample-detector distance of 110 mm in a coupled $\theta/2\theta$ scan from 0° to 15°. Diffraction patterns were background corrected by subtracting a measurement of the bare substrate.

Supporting Information

Supporting Information is available from the Wiley Online Library or from the author.

Acknowledgements

The authors would like to kindly thank Prof. Uwe Bunz for providing access to the device fabrication facilities and Prof. Markus Motzkus for access to the ultrafast laser lab. The authors thank Edinburgh Instruments for PL data of PCBM. The authors thank the DFG (VA 991/2-1) for support. A.W. thanks Dr. Luis Perez-Lustres and Dr. Tiago Buckup for help with data analysis. This project received funding from the European Research Council (ERC) under the European Union's Horizon 2020 research and innovation programme (ERC Grant Agreement No. 714067, ENERGYMAPS) and ERC Grant Agreement No. 639750, VIBCONTROL.

Conflict of Interest

The authors declare no conflict of interest.

Keywords

device stability, energy transfer, organic photovoltaics, small molecule donor, transient absorption spectroscopy

Received: September 8, 2019
Revised: October 17, 2019
Published online: November 20, 2019

[1] B. Fan, D. Zhang, M. Li, W. Zhong, Z. Zeng, L. Ying, F. Huang, Y. Cao, *Sci. China Chem.* **2019**, *62*, 746.
[2] J. Yuan, Y. Zhang, L. Zhou, G. Zhang, H.-L. Yip, T.-K. Lau, X. Lu, C. Zhu, H. Peng, P. A. Johnson, M. Leclerc, Y. Cao, J. Ulanski, Y. Li, Y. Zou, *Joule* **2019**, *3*, 1140.
[3] M. Hermenau, M. Riede, K. Leo, *Stability and Degradation of Organic and Polymer Solar Cells*, John Wiley & Sons, Ltd, Chichester, UK **2012**, pp. 109–142.
[4] B. Walker, C. Kim, T.-Q. Nguyen, *Chem. Mater.* **2011**, *23*, 470.
[5] Y. Chen, X. Wan, G. Long, *Acc. Chem. Res.* **2013**, *46*, 2645.
[6] J. E. Coughlin, Z. B. Henson, G. C. Welch, G. C. Bazan, *Acc. Chem. Res.* **2014**, *47*, 257.
[7] Y. Lin, Y. Li, X. Zhan, *Chem. Soc. Rev.* **2012**, *41*, 4245.
[8] L. Gao, Z.-G. Zhang, H. Bin, L. Xue, Y. Yang, C. Wang, F. Liu, T. P. Russell, Y. Li, *Adv. Mater.* **2016**, *28*, 8288.
[9] W. Zhao, D. Qian, S. Zhang, S. Li, O. Inganäs, F. Gao, J. Hou, *Adv. Mater.* **2016**, *28*, 4734.
[10] W. Zhao, S. Li, H. Yao, S. Zhang, Y. Zhang, B. Yang, J. Hou, *J. Am. Chem. Soc.* **2017**, *139*, 7148.
[11] H. Feng, N. Qiu, X. Wang, Y. Wang, B. Kan, X. Wan, M. Zhang, A. Xia, C. Li, F. Liu, H. Zhang, Y. Chen, *Chem. Mater.* **2017**, *29*, 7908.
[12] C. Sun, F. Pan, H. Bin, J. Zhang, L. Xue, B. Qiu, Z. Wei, Z.-G. Zhang, Y. Li, *Nat. Commun.* **2018**, *9*, 743.
[13] B. Kan, J. Zhang, F. Liu, X. Wan, C. Li, X. Ke, Y. Wang, H. Feng, Y. Zhang, G. Long, R. H. Friend, A. A. Bakulin, Y. Chen, *Adv. Mater.* **2018**, *30*, 1704904.
[14] J. Hou, O. Inganäs, R. H. Friend, F. Gao, *Nat. Mater.* **2018**, *17*, 119.
[15] Q. Zhang, B. Kan, F. Liu, G. Long, X. Wan, X. Chen, Y. Zuo, W. Ni, H. Zhang, M. Li, Z. Hu, F. Huang, Y. Cao, Z. Liang, M. Zhang, T. P. Russell, Y. Chen, *Nat. Photonics* **2015**, *9*, 35.
[16] Y. Sun, G. C. Welch, W. L. Leong, C. J. Takacs, G. C. Bazan, A. J. Heeger, *Nat. Mater.* **2012**, *11*, 44.
[17] B. Qiu, L. Xue, Y. Yang, H. Bin, Y. Zhang, C. Zhang, M. Xiao, K. Park, W. Morrison, Z.-G. Zhang, Y. Li, *Chem. Mater.* **2017**, *29*, 7543.
[18] D. Deng, Y. Zhang, J. Zhang, Z. Wang, L. Zhu, J. Fang, B. Xia, Z. Wang, K. Lu, W. Ma, Z. Wei, *Nat. Commun.* **2016**, *7*, 13740.
[19] A. J. Pearson, P. E. Hopkinson, E. Couderc, K. Domanski, M. Abdi-Jalebi, N. C. Greenham, *Org. Electron.* **2016**, *30*, 225.
[20] L. E. Garner, V. Nellissery Viswanathan, D. H. Arias, C. P. Brook, S. T. Christensen, A. J. Ferguson, N. Kopidakis, B. W. Larson, Z. R. Owczarczyk, J. R. Pfeilsticker, P. C. Ramamurthy, S. H. Strauss, O. V. Boltalina, W. A. Braunecker, *J. Mater. Chem. A* **2018**, *6*, 4623.
[21] W. R. Mateker, T. Heumueller, R. Cheacharoen, I. T. Sachs-Quintana, M. D. McGehee, J. Warnan, P. M. Beaujuge, X. Liu, G. C. Bazan, *Chem. Mater.* **2015**, *27*, 6345.
[22] R. A. Street, D. M. Davies, *Appl. Phys. Lett.* **2013**, *102*, 043305.
[23] Z. Shang, T. Heumueller, R. Prasanna, G. F. Burkhard, B. D. Naab, Z. Bao, M. D. McGehee, A. Salleo, *Adv. Energy Mater.* **2016**, *6*, 1601149.
[24] A. Seemann, T. Sauermann, C. Lungenschmied, O. Armbruster, S. Bauer, H.-J. Egelhaaf, J. Hauch, *Sol. Energy* **2011**, *85*, 1238.
[25] H.-H. Liao, C.-M. Yang, C.-C. Liu, S.-F. Horng, H.-F. Meng, J.-T. Shy, *J. Appl. Phys.* **2008**, *103*, 104506.
[26] A. Weu, J. A. Kress, F. Paulus, D. Becker-Koch, V. Lami, A. A. Bakulin, Y. Vaynzof, *ACS Appl. Energy Mater.* **2019**, *2*, 1943.
[27] E. M. Speller, A. J. Clarke, N. Aristidou, M. F. Wyatt, L. Francàs, G. Fish, H. Cha, H. K. H. Lee, J. Luke, A. Wadsworth, A. D. Evans, I. McCulloch, J.-S. Kim, S. A. Haque, J. R. Durrant, S. D. Dimitrov, W. C. Tsoi, Z. Li, *ACS Energy Lett.* **2019**, *4*, 846.
[28] A. Perthué, I. Fraga Domínguez, P. Verstappen, W. Maes, O. J. Dautel, G. Wantz, A. Rivaton, *Sol. Energy Mater. Sol. Cells* **2018**, *176*, 336.
[29] W. R. Mateker, M. D. McGehee, *Adv. Mater.* **2017**, *29*, 1603940.
[30] N. Li, J. D. Perea, T. Kassar, M. Richter, T. Heumueller, G. J. Matt, Y. Hou, N. S. Güldal, H. Chen, S. Chen, S. Langner, M. Berlinghof, T. Unruh, C. J. Brabec, *Nat. Commun.* **2017**, *8*, 14541.
[31] Q. Liu, J. Toudert, F. Liu, P. Mantilla-Perez, M. M. Bajo, T. P. Russell, J. Martorell, *Adv. Energy Mater.* **2017**, *7*, 1701201.
[32] J. W. Rumer, I. McCulloch, *Mater. Today* **2015**, *18*, 425.
[33] L. Zhang, B. Lin, B. Hu, X. Xu, W. Ma, *Adv. Mater.* **2018**, *30*, 1800343.
[34] H. Cha, J. Wu, A. Wadsworth, J. Nagitta, S. Limbu, S. Pont, Z. Li, J. Searle, M. F. Wyatt, D. Baran, J.-S. Kim, I. McCulloch, J. R. Durrant, *Adv. Mater.* **2017**, *29*, 1701156.
[35] H. K. H. Lee, A. M. Telford, J. A. Röhr, M. F. Wyatt, B. Rice, J. Wu, A. de Castro Maciel, S. M. Tuladhar, E. Speller, J. McGettrick, J. R. Searle, S. Pont, T. Watson, T. Kirchartz, J. R. Durrant, W. C. Tsoi, J. Nelson, Z. Li, *Energy Environ. Sci.* **2018**.
[36] A. Perthué, T. Gorisse, H. S. Silva, C. Lombard, D. Bégué, P. Hudhomme, B. Pépin-Donat, A. Rivaton, G. Wantz, *J. Mater. Res.* **2018**, *33*, 1868.
[37] M. O. Reese, A. M. Nardes, B. L. Rupert, R. E. Larsen, D. C. Olson, M. T. Lloyd, S. E. Shaheen, D. S. Ginley, G. Rumbles, N. Kopidakis, *Adv. Funct. Mater.* **2010**, *20*, 3476.
[38] M. Hermenau, M. Riede, K. Leo, S. A. Gevorgyan, K. Norrman, *Sol. Energy Mater. Sol. Cells* **2011**, *95*, 1268.
[39] M. Hermenau, K. Leo, M. Riede, *Proc. SPIE* **2010**, *7722*, 77220K.

[40] R. Lessmann, Z. Hong, S. Scholz, B. Maennig, M. K. Riede, K. Leo, *Org. Electron.* **2010**, *11*, 539.
[41] F. C. Krebs, K. Norrman, *Prog. Photovoltaics* **2007**, *15*, 697.
[42] M. P. de Jong, L. J. van IJzendoorn, M. J. A. de Voigt, *Appl. Phys. Lett.* **2000**, *77*, 2255.
[43] K. W. Wong, H. L. Yip, Y. Luo, K. Y. Wong, W. M. Lau, K. H. Low, H. F. Chow, Z. Q. Gao, W. L. Yeung, C. C. Chang, *Appl. Phys. Lett.* **2002**, *80*, 2788.
[44] M. Jørgensen, K. Norrman, F. C. Krebs, *Sol. Energy Mater. Sol. Cells* **2008**, *92*, 686.
[45] A. K. K. Kyaw, D. H. Wang, V. Gupta, J. Zhang, S. Chand, G. C. Bazan, A. J. Heeger, *Adv. Mater.* **2013**, *25*, 2397.
[46] B. Kan, M. Li, Q. Zhang, F. Liu, X. Wan, Y. Wang, W. Ni, G. Long, X. Yang, H. Feng, Y. Zuo, M. Zhang, F. Huang, Y. Cao, T. P. Russell, Y. Chen, *J. Am. Chem. Soc.* **2015**, *137*, 3886.
[47] K. Yamamoto, M. Shahiduzzaman, A. Yamada, T. Takaya, T. Chikamatsu, T. Koganezawa, M. Karakawa, T. Kuwabara, K. Takahashi, T. Taima, *Org. Electron.* **2018**, *63*, 47.
[48] Y. Wang, M. Chang, B. Kan, X. Wan, C. Li, Y. Chen, *ACS Appl. Energy Mater.* **2018**, *1*, 2150.
[49] N. Liang, D. Meng, Z. Ma, B. Kan, X. Meng, Z. Zheng, W. Jiang, Y. Li, X. Wan, J. Hou, W. Ma, Y. Chen, Z. Wang, *Adv. Energy Mater.* **2017**, *7*, 1601664.
[50] R. Cheacharoen, W. R. Mateker, Q. Zhang, B. Kan, D. Sarkisian, X. Liu, J. A. Love, X. Wan, Y. Chen, T.-Q. Nguyen, G. C. Bazan, M. D. McGehee, *Sol. Energy Mater. Sol. Cells* **2017**, *161*, 368.
[51] J. Min, X. Jiao, V. Sgobba, B. Kan, T. Heumüller, S. Rechberger, E. Spiecker, D. M. Guldi, X. Wan, Y. Chen, H. Ade, C. J. Brabec, *Nano Energy* **2016**, *28*, 241.
[52] T. Heumueller, W. R. Mateker, A. Distler, U. F. Fritze, R. Cheacharoen, W. H. Nguyen, M. Biele, M. Salvador, M. Von Delius, H. J. Egelhaaf, M. D. McGehee, C. J. Brabec, *Energy Environ. Sci.* **2016**, *9*, 247.
[53] H. K. H. Lee, A. M. Telford, J. A. Röhr, M. F. Wyatt, B. Rice, J. Wu, A. de Castro Maciel, S. M. Tuladhar, E. Speller, J. McGettrick, J. R. Searle, S. Pont, T. Watson, T. Kirchartz, J. R. Durrant, W. C. Tsoi, J. Nelson, Z. Li, *Energy Environ. Sci.* **2018**, *11*, 417.
[54] W. Greenbank, L. Hirsch, G. Wantz, S. Chambon, *Appl. Phys. Lett.* **2015**, *107*, 263301.
[55] W. Greenbank, N. Rolston, E. Destouesse, G. Wantz, L. Hirsch, R. Dauskardt, S. Chambon, *J. Mater. Chem. A* **2017**, *5*, 2911.
[56] W. Greenbank, L. Hirsch, S. Chambon, *Sol. Energy Mater. Sol. Cells* **2018**, *178*, 8.
[57] Y. Sevinchan, P. E. Hopkinson, A. A. Bakulin, J. Herz, M. Motzkus, Y. Vaynzof, *Adv. Mater. Interfaces* **2016**, *3*, 1500616.
[58] C. Hinzmann, O. Magen, Y. J. Hofstetter, P. E. Hopkinson, N. Tessler, Y. Vaynzof, *ACS Appl. Mater. Interfaces* **2017**, *9*, 6220.
[59] A. Tournebize, P.-O. Bussière, P. Wong-Wah-Chung, S. Thérias, A. Rivaton, J.-L. Gardette, S. Beaupré, M. Leclerc, *Adv. Energy Mater.* **2013**, *3*, 478.
[60] J. Razzell-Hollis, J. Wade, W. C. Tsoi, Y. Soon, J. Durrant, J. S. Kim, *J. Mater. Chem. A* **2014**, *2*, 20189.
[61] I. Fraga Domínguez, P. D. Topham, P.-O. Bussière, D. Bégué, A. Rivaton, *J. Phys. Chem. C* **2015**, *119*, 2166.
[62] M. Manceau, A. Rivaton, J.-L. Gardette, S. Guillerez, N. Lemaître, *Sol. Energy Mater. Sol. Cells* **2011**, *95*, 1315.
[63] G. J. Hedley, A. Ruseckas, I. D. W. Samuel, *Chem. Rev.* **2017**, *117*, 796.
[64] O. Ostroverkhova, *Chem. Rev.* **2016**, *116*, 13279.
[65] S. M. Menke, R. J. Holmes, *Energy Environ. Sci.* **2014**, *7*, 499.
[66] E. M. Speller, A. J. Clarke, J. Luke, H. K. H. Lee, J. R. Durrant, N. Li, T. Wang, H. C. Wong, J.-S. Kim, W. C. Tsoi, Z. Li, *J. Mater. Chem. A* **2019**, *7*, 23361.
[67] E. T. Hoke, I. T. Sachs-Quintana, M. T. Lloyd, I. Kauvar, W. R. Mateker, A. M. Nardes, C. H. Peters, N. Kopidakis, M. D. McGehee, *Adv. Energy Mater.* **2012**, *2*, 1351.
[68] C. Yan, S. Barlow, Z. Wang, H. Yan, A. K.-Y. Jen, S. R. Marder, X. Zhan, *Nat. Rev. Mater.* **2018**, *3*, 18003.
[69] N. Gasparini, A. Salleo, I. McCulloch, D. Baran, *Nat. Rev. Mater.* **2019**, *4*, 229.
[70] A. Weu, T. R. Hopper, V. Lami, J. A. Kreß, A. A. Bakulin, Y. Vaynzof, *Chem. Mater.* **2018**, *30*, 2660.